Separation Science and Technology
Publication details, including instructions for authors and subscription information:
http://www.informaworld.com/smpp/title~content=t713708471

MAGNUS SEPARATION

P. C. Rem[a]; N. Fraunholcz[a]; E. A. Schokker[a]
[a] Department of Applied Earth Sciences, Delft University of Technology, Delft, The Netherlands

Online publication date: 12 February 2002

To cite this Article Rem, P. C. , Fraunholcz, N. and Schokker, E. A.(2002) 'MAGNUS SEPARATION', Separation Science and Technology, 37: 16, 3647 — 3660
To link to this Article: DOI: 10.1081/SS-120014824
URL: http://dx.doi.org/10.1081/SS-120014824

MARCEL DEKKER, INC. • 270 MADISON AVENUE • NEW YORK, NY 10016

SEPARATION SCIENCE AND TECHNOLOGY
Vol. 37, No. 16, pp. 3647–3660, 2002

MAGNUS SEPARATION

P. C. Rem,* N. Fraunholcz, and E. A. Schokker

Department of Applied Earth Sciences, Delft University of Technology, Mijnbouwstraat 120, 2628 RX Delft, The Netherlands

ABSTRACT

The Magnus effect, i.e., the lift force, which is observed when a spinning body moves through a fluid at right angles to its axis of rotation, can be used to separate metal particles from a mixture. The necessary selective rotation of the metal particles is brought about by the action of a fast-spinning magnet rotor, of the same kind that is used for eddy current separation. Experiments show that metal particles with screen sizes from 500 μm to 10 mm can be concentrated from a slurry fed on top of the rotor. A potential application of wet Magnus separation is the recovery of aluminum, copper, and zinc from the bottom ashes of (municipal) solid waste incinerators. Mixtures of a more narrow size range, from 500 μm to 2 mm, can also be treated dry. Dry Magnus separation may be interesting for the recovery of precious metals from dry alluvial deposits, as it combines high capacity with low cost.

Key Words: Metals; Recycling; Fluid mechanics

*Corresponding author. Fax: +31-15-2782836; E-mail: p.c.rem@ta.tudelft.nl

DOI: 10.1081/SS-120014824
0149-6395 (Print); 1520-5754 (Online)

www.dekker.com

MARCEL DEKKER, INC. • 270 MADISON AVENUE • NEW YORK, NY 10016

INTRODUCTION

Today, physical separation and electronic sortation technologies offer a wide choice of processes for the recovery of metals from solid waste. Nevertheless, waste fractions with low concentrations of metals and particle sizes in the range from 500 μm to 10 mm are difficult to treat. An example is the bottom ash produced by incinerators of solid waste, which often contains a little percent of nonferrous metals, such as aluminum, copper, and zinc. Conventional dry eddy current separation is applied only to fractions larger than 10 mm, in this way recovering less than half of the nonferrous metals that are available in bottom ash. In the year 2000, 7 kt were recovered out of an estimated total of 25 kt nonferrous present in the Dutch bottom ash.[1] For comparison, the total aluminum content of waste and end-of-life products for the same year was estimated at 150 kt in the Netherlands.[2]

The newly discovered process of Magnus separation[3,4] consists of making the feed particles fall close to a fast-spinning magnet. The effect of the rotor is to create a selective rotation of the metal particles, by means of a magnetic coupling between the eddy currents induced in the metal and the rotating magnetic field. The metal particles are then deflected by a hydrodynamic or aerodynamic lift force, which is known as the Magnus effect[5] (Fig. 1). Like conventional eddy current separation, the Magnus process is selective for well-conducting metals, but due to the intermediate interaction with the fluid, the separation force is not as strongly dependent on the particle size, so that the separation is effective for fine

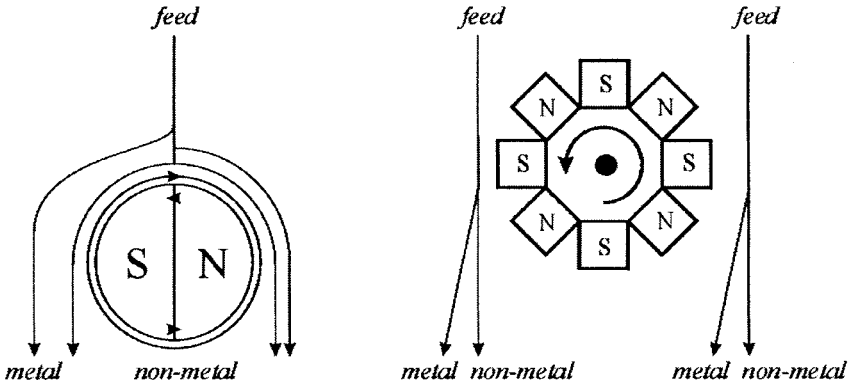

Figure 1. Principle of wet (left) and dry (right) Magnus processes. The feed can be introduced on top or on either side of the magnet rotor. If the rotor spins counterclockwise, the metal particles (thick arrows) will rotate clockwise and drift to the left of the feedstream.

fractions as well, from about 500 μm particles upward. Since the feed is introduced as a stream without contact with a conveyor belt and feeding the particles as a monolayer is not necessary, the capacity of Magnus separators is of the order of 10 t/hr or more per meter length of the rotor, even at small particle sizes.

MAGNUS SEPARATION

It was discovered early in the history of fluid dynamics that particles, which rotate around a horizontal axis, do not settle vertically in a fluid,[6,7] as particles without spin will, on average. The rotational motion causes an asymmetry in the flow around such particles,[5] making them drift sideward. Figure 2 shows a simple experiment in which copper cylinders roll from a ramp into a vessel filled with water.

The conventional way of describing the linear motion of a spinning particle in a fluid is to decompose the force of the fluid on the particle into a component F_D (the drag) that is parallel to the relative motion of the fluid and the particle,

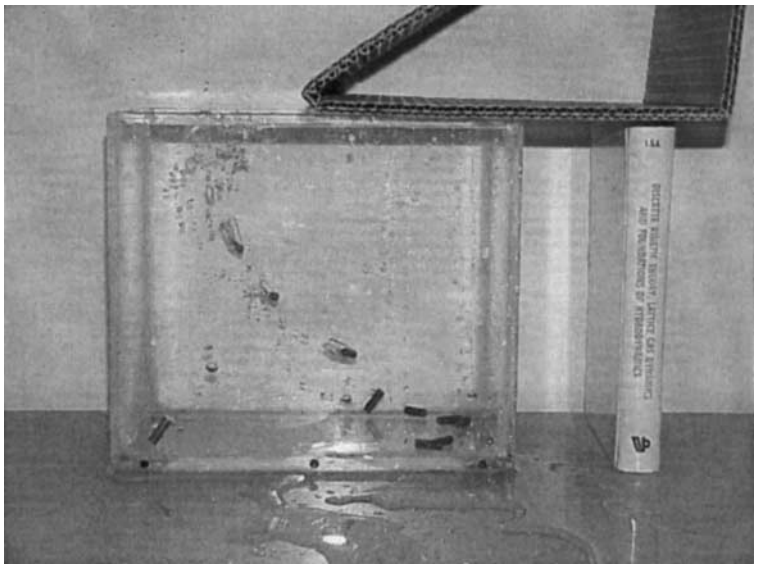

Figure 2. Magnus effect on 6-mm diameter copper cylinders in water reverses the horizontal motion of the cylinders from left to right.

and a second component F_L (the lift), which by definition is at right angles to the relative motion (Fig. 3).

Both components of the force are usually correlated to the kinetic energy of the fluid per unit volume, $\rho v^2/2$, as observed by the particle, and a characteristic area A of the particle, most often the cross-sectional area that is presented towards the flow:

$$F_D = c_D \frac{\rho v^2}{2} A, \tag{1}$$

$$F_L = c_L \frac{\rho v^2}{2} A. \tag{2}$$

In general, the coefficients of drag and lift, c_D and c_L, depend on two dimensionless numbers: the Reynolds number of the flow, *Re*, and *Ro*, the ratio of the surface velocity of the particle to its linear velocity. If D is a characteristic dimension of the particle and η is the dynamic viscosity of the fluid, *Re* and *Ro* are expressed as

$$Re = \frac{\rho v D}{\eta}, \tag{3}$$

$$Ro = \frac{\Omega D}{2v}. \tag{4}$$

Here Ω is the angular velocity of the particle. Both c_D and c_L are usually of the order of 1, with some large values being measured for cylinders.[8] It has been noted by Tritton[5] that the coefficient of lift seems to be rather independent of the Reynolds number, at least for Reynolds numbers exceeding 1500. So far, no measurements appear to have been done outside the turbulent region. This means that the known data relate to particles exceeding about 2 mm in diameter.

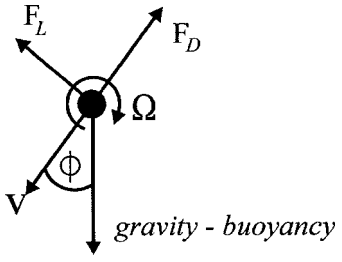

Figure 3. Force diagram for a particle that rotates at angular velocity Ω while settling with linear velocity v with respect to a fluid.

The most simple situation to analyze is that of a spinning particle, settling in a fluid at constant angular and linear velocities. The balance of forces (Fig. 3) shows that such a particle traces a straight line through the fluid, at an angle

$$\phi = \arctan(c_L/c_D) \tag{5}$$

with the vertical. The terminal velocity of the particle is given by

$$v = \sqrt{\frac{2(\rho_s - \rho)Vg}{c\rho A}}, \tag{6}$$

where ρ_s is the density of the particle, g is the acceleration of gravity, and $c = \sqrt{c_D^2 + c_L^2}$. One of the striking features of the available data presented in Fig. 4 is the strong dependence of the drift angle on the particle shape. For small values of *Ro*, the drift angle shows a steep rise, approximating a constant for larger values of *Ro*.

The situation of steady-state settling comes close to the wet Magnus process, where particles are almost always near their terminal velocity. For example, a rotating particle of 10 mm diameter has a terminal velocity in water of less than 1 m/sec and reaches a substantial fraction of this velocity within a drop of about 0.05 m. Most particles, except for those with very round shapes, lose their angular velocity rapidly as they move out of the field of the rotor. As a result, the angular velocities of particles in a wet Magnus process can be approximated by assuming a balance between the magnetic torque of the rotor and the counter-acting drag torque of the water.

In air, the angular velocity of metal particles is not so much bounded by the resistance with the air but by the frequency of the magnetic field of the rotor. Even very small particles keep a large fraction of the angular momentum imparted by the rotor field after a drop of several meters through the air. In the dry Magnus process (Fig. 1), the particles first acquire a high angular velocity while passing the rotor at relatively low speed. For a successful separation, the lift force must then reach some fraction of the gravity on the particle, in order to deflect the metal particles from the vertical trajectory followed by the nonmetals in the feed. Since the forces of lift and drag are similar in size, this implies that the metal particles should arrive at a significant fraction of their terminal velocities, before being separated from the mainstream. For this reason, the separation in air is limited to particles of smaller sizes than in water.

PARTICLE ROTATION

Metal particles start to spin when they are subjected to the field of a rotating magnet. The spinning motion is caused by the onset of eddy currents inside

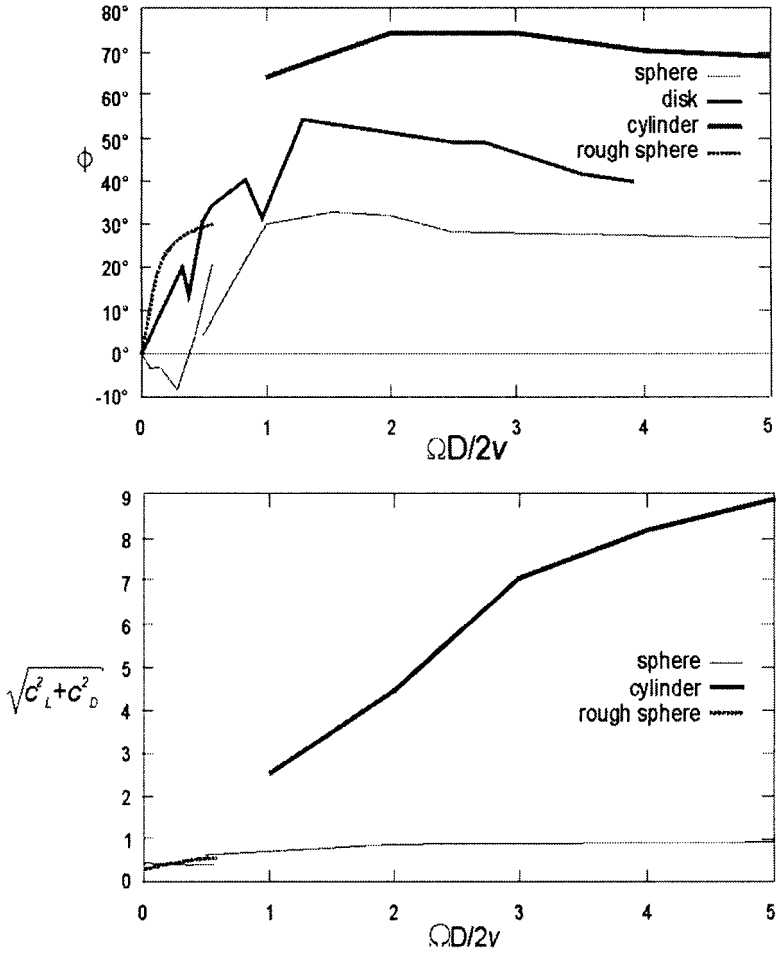

Figure 4. Drift angle ϕ and $c = \sqrt{c_{\mathrm{D}}^2 + c_{\mathrm{L}}^2}$ for spherical and cylindrical particles computed from literature data[7–10] for high Reynolds numbers ($Re = 10^4 - 10^5$). Also shown are preliminary measurements for disks by the authors for $Re = 300 - 700$ and $Re = 30{,}000$. Data for cylinders relate to a rotation around the axis of symmetry, whereas data for disks refer to a rotation axis within the plane of the disks.

the particles, which turn the particle into a small electromagnet that tries to align with the field of the rotor. The axis of the rotor in Magnus separation is oriented horizontally, so that the metal particles start to spin around a horizontal axis as well (Fig. 5). The rotor not only makes the particles spin but also accelerates them in a direction, which is between radially outward and tangential with the surface

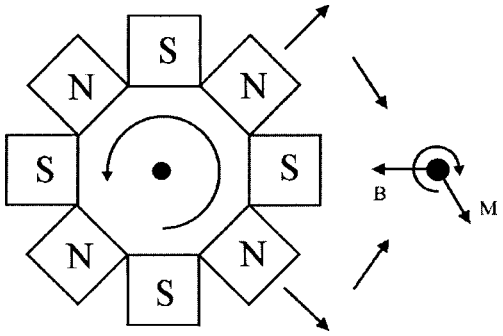

Figure 5. Magnetic field **B** at several positions near a magnet rotor, showing the apparent clockwise rotation of the field vector at the position of the particle and the magnetic moment **M** of the particle resulting from induced eddy currents. Note that the particle magnetic moment rotates at the same angular velocity as the field vector, lagging behind by between 90 and 180°.

velocity of the rotor. This direct force is used in conventional eddy current separation and is generally of minor importance in Magnus separation.

Both the force and the torque can be calculated analytically for particles of elementary shapes. As the feed particles will never be very close to the surface of the magnet, the interaction with the rotor can be simplified by considering only the principal multipole component of the rotor field. For a magnet rotor with k North poles, an outer radius R_m, and spinning at angular velocity ω_m, the field in cylindrical coordinates (r, ϕ) with respect to the axis of rotation of the rotor is:

$$\mathbf{B} = \begin{pmatrix} B_r \\ B_\phi \end{pmatrix} \cong b\left(\frac{R_m}{r}\right)^{k+1} \begin{pmatrix} \cos k(\phi - \omega_m t) \\ \sin k(\phi - \omega_m t) \end{pmatrix}. \tag{7}$$

The expression shows that a stationary particle at some point (r, ϕ) experiences a field vector of constant magnitude $\hat{B} = b(R_m/r)^{k+1}$ revolving at angular velocity $-k\omega_m$ (Fig. 5). The value of b is typically 0.6 T for modern FeNdB magnets, provided R_m is the surface radius of the magnetic material. Rotor speeds vary from 3000 rpm (or about 300 rad/sec) for a multipole rotor of 300 mm diameter to 10,000 rpm (or about 1000 rad/sec) for a dipole rotor of 100 mm diameter, resulting in a surface velocity of the rotor of about 50 m/sec. While a particle moves through the magnetic field, it experiences changes of size and orientation of the field due to its own translational and rotational motion as well as due to the rotation of the rotor. Since the surface velocity of the rotor will generally exceed the particle velocity by more than an order of magnitude, the force and torque

depend only on the position, orientation, and angular velocity of the particles. If the particle itself is spinning with some angular velocity Ω, it perceives a field of the same size as a stationary particle but now rotating at an apparent angular velocity $-k\omega_{\mathrm{m}} - \Omega$. The magnetic torque makes the particle spin in the same direction as the magnetic field. This has the effect that, as the particle rotation increases, i.e., $\Omega \rightarrow -k\omega_{\mathrm{m}}$, the apparent field rotation slows down and the torque and force acting on the particle vanish accordingly.

A major simplification results from the fact that the diameter of particles in a Magnus separation process is always small with respect to the magnetic wavelength $2\pi R_{\mathrm{m}}/(k+1)$ of the rotor. For this case, the existing theory of eddy current separation[3] gives an expression for the magnetic dipole moment $\mathbf{M}$ for nonferrous particles of regular shapes such as spheres, disks, and cylinders in various orientations with respect to the axis of the rotor:

$$\mathbf{M} = -\frac{V}{\mu_0}\left[R(\mu_0(k\omega_{\mathrm{m}}+\Omega)\sigma d^2)\begin{pmatrix} B_r \\ B_\phi \end{pmatrix} + I(\mu_0(k\omega_{\mathrm{m}}+\Omega)\sigma d^2)\begin{pmatrix} B_\phi \\ -B_r \end{pmatrix}\right]. \tag{8}$$

In this expression V and σ are the volume of the particle and its electrical conductivity, respectively, and $R(\xi)$ and $I(\xi)$ are dimensionless functions, for which approximations in terms of rational functions are tabulated in Table 1.

Table 1. Parameters Defining the Magnetic Interaction for Particles of Several Shapes and Parallel (∥) or Perpendicular (⊥) Orientations of Their Axis of Symmetry with Respect to the Axis of the Rotor

Shape	$(R(\xi),\mathrm{I}(\xi))$	D	c_{m}	γ
Sphere	$\frac{21(\xi^2,42\xi)}{20(1764+\xi^2)}$	D	1/40	1/4
Cylinder ∥	$\frac{3(\xi^2,24\xi)}{2(576+\xi^2)}$	D	1/16	1/2
Cylinder ⊥	$\frac{9(\xi^2,24\xi)}{8(576+\xi^2)}$	D	3/64	$9D^2/16L^2$
Disk ∥	$\frac{(\xi^2,12\xi)}{(144+\xi^2)}$	δ	1/12	$2\delta^2/3D^2$
Disk ⊥	$\frac{(0.6\pi\delta\xi^2/D,16\xi)}{4(256+(0.6\pi\delta)^2\xi^2/D^2)}$	D	1/64	1/4

D: diameter, L: length, δ: thickness.

The dimensionless group $\sqrt{\mu_0(k\omega_m + \Omega)\sigma d^2}$ is the ratio of the relevant particle dimension d to the skin depth, i.e., the depth to which the magnetic field of the rotor is able to penetrate the particle (Table 2). The torque on the particle follows directly from its magnetic moment:

$$\mathbf{T}_m = \mathbf{M} \times \mathbf{B} = -\frac{\hat{B}^2 V}{\mu_0} I(\xi)\mathbf{e}_z. \tag{9}$$

Since the gradient of the rotor field (again in cylinder coordinates) is

$$\nabla\mathbf{B} = -\frac{k+1}{r}\begin{pmatrix} B_r & B_\phi \\ B_\phi & -B_r \end{pmatrix}, \tag{10}$$

the direct magnetic force is given by

$$\mathbf{F}_m = \mathbf{M}\cdot\nabla\mathbf{B} = \frac{(k+1)\hat{B}^2 V}{\mu_0 r}\begin{pmatrix} R(\xi) \\ I(\xi) \end{pmatrix}. \tag{11}$$

The speed of rotation Ω of the metal particles in a Magnus process is found by integration of the balance of angular momentum:

$$J\Omega = T_m - T_d. \tag{12}$$

For metal particles with d less than 10 mm, the factor I in T_m reduces to a linear function of ω_m:

$$T_m = -c_m(k\omega_m + \Omega)\hat{B}^2\sigma d^2 V. \tag{13}$$

The coefficient c_m depends on the shape and orientation of the particle (Table 1).

The rotational drag T_d of the fluid is described by an even simpler expression: for not too low Reynolds numbers ($Re > 300$):

$$T_d = c_T D^5 \rho|\Omega|\Omega. \tag{14}$$

Table 2. Specific Density and Electrical Conductivity of Some Metals and Alloys

Alloy	Density, ρ_s (kg/m^3)	Conductivity, σ (1/Ω m)	σ/ρ_s (m^2/Ω kg)
Aluminum 3003	2,700	27×10^6	10,000
Copper	8,900	56×10^6	6,300
Zinc	7,100	17×10^6	2,400
Yellow brass	8,500	15×10^6	1,750
Lead	11,400	5×10^6	440
Solder 50–50	8,900	7×10^6	800

Table 3. Calculated Coefficients for the Rotor Torque and Measured Values for the Drag Torque Coefficient for Particles of Several Shapes

Particle Definition	c_T	$C = c_m V/c_T D^3$
Rough sphere ($Re = 300–700$)	0.007	1.9
Smooth sphere ($Re = 3 \times 10^6$)[10]	0.0008	16
Rough cylinder ($Re = 500–700$, $L/D = 3$)	0.008 L/D	6
Smooth cylinder ($Re = 2 \times 10^6$, $L/D = 5$)[8]	0.0012 L/D	40
Disk ($Re = 300–30{,}000$, $D/\delta = 3.5–4$)	0.03	0.4 δ/D

The data are for cylinders rotating around their axis of symmetry and disks rotating around an axis perpendicular to their axis of symmetry.

Here again, c_T is a coefficient that depends on the shape and orientation of the particle (see Table 3 for typical values).

Surprisingly, the expressions for T_m and T_d imply that within the size ranges indicated, the particle spin does not depend on the size of the particle, but only on its shape and orientation, since J, T_m, and T_d are all proportional to the fifth power of the particle size.

Evaluation of the three terms of the equation of motion shows that in water the balance between rotor torque and drag is realized almost instantly (20–100 msec), except for perfectly round particles with a smooth surface. Furthermore, Ω is bounded to low values by the resistance with water, so that the spin of the metal particles can be estimated by setting $\Omega \ll k\omega_m$ and $T_m = T_d$, or (see Table 3 for typical values of C)

$$|\Omega| = \hat{B}\sqrt{Ck|\omega_m|\sigma/\rho}. \tag{15}$$

Assuming that the field of the rotor $\hat{B}$ is about 0.1 T, we find that a typical rotation speed for the metal particles in water is 100 rad/sec.

For a dry Magnus separation, the particles first pass the rotor at low velocity to pick up rotational speed. Since the time in passing the field region is short, the rotational drag can be neglected for this part of the particle trajectory. Assuming that the particle passes the rotor at some velocity v_0, with $\hat{B}_0$ being the maximum field strength encountered at $r = r_0$, the final angular velocity is estimated as ($n!! = n(n-2)(n-4)\cdots$):

$$\Omega_0 = -k\omega_m(1 - e^{-v^*/v_0}), \quad v^* = \frac{\pi(2k-1)!!}{(2k)!!}\gamma\hat{B}_0^2 r_0 \frac{\sigma}{\rho_s}. \tag{16}$$

The shape and orientation factor $\gamma = c_m\rho_s V d^2/J$ (Table 1).

EXPERIMENTS

Table 4 shows some results of experiments with single particles falling next to an 18-pole magnetic rotor in air. The measured horizontal deviation of the particle is an average of a large number of identical particles. The particles were dropped from a point 150 mm above the axis of the rotor and collected at a point 1.5 m below the axis.

Experiments were conducted with the 2–6 mm fraction of bottom ash from the municipal waste incinerator at Alkmaar, the Netherlands (Fig. 6). The original material sample was screened wet and processed with a cross-belt magnetic separator to remove most of the magnetic material from the feed. This preparation step is necessary to prevent sticking of magnetic material to the shell protecting the rotor of the Magnus separator. The material was then fed one particle at a time through a metal detector and the resulting nonferrous fraction was separated according to density in a heavy liquid to separate aluminum from copper and zinc. The metals were colored with a spray-paint and recombined with the nonmagnetic fraction. This fraction was then passed through the separator and collected in a row of compartments. Table 5 shows the grade and recovery in the metal concentrate as a function of the splitter point, i.e., the point between tailings compartments and product compartments. At a commercially attractive grade of 80%, the metal recovery is over 70%.

So far, aluminum from the fine fractions of bottom ash has never been recycled. This raises the question whether aluminum of this type can be smelted in the same way as for the coarser fractions, and whether the yield of the smelter will not be too low. Table 6 shows the recovery of metallic aluminum in laboratory tests, showing that the material has a standard behavior in the smelt. For copper and zinc, fine material is recycled routinely, e.g., in the recycling of wire and cable.

Table 4. Comparison of Measured and Simulated Horizontal Deviations for Single Disk- and Cylinder-Shaped Particles Falling Next to an 18-Pole Magnet Rotor with $\omega_m = 314\,\text{rad/sec}$, $\hat{B}_0 = 0.24\,\text{T}$, and $r_0 = 0.154\,\text{m}$

Metal	Shape	Diameter (mm)	Thickness (mm)	Simulated (mm)	Measured (mm)
Aluminum	Disk	3.2	0.5	238	207 ± 14
Copper	Disk	3.2	0.5	84	84 ± 8
Copper	Disk	3.2	0.2	185	177 ± 16
Copper	Disk	1.6	0.1	244	281 ± 11
Aluminum	Cylinder	1.0	1.0	120	125 ± 14

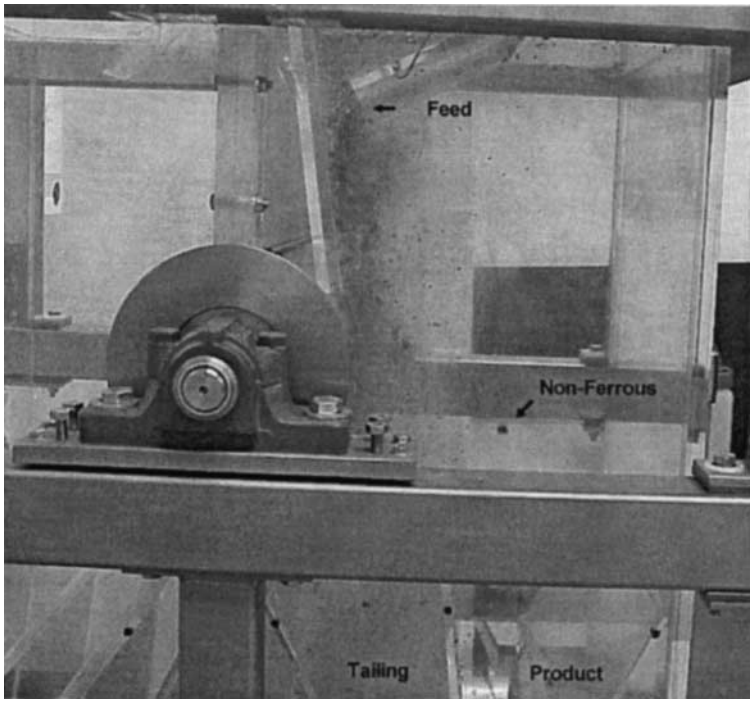

Figure 6. Feeding of bottom ash to the Delft pilot Magnus separator.

Table 5. Grade–Recovery Data for the 2–6 mm Nonmagnetic Fraction of the Alkmaar Bottom Ash

Splitter Setting	Grade (%)	Recovery (%)
None	6.1	100.0
12	28.5	93.3
11	56.6	88.5
10	89.4	71.6
9	93.9	60.4
7	100.0	21.1

Recovery is defined as the mass % of the nonferrous metals in the feed that report to the metal concentrate (product). Grade is defined as the mass % of nonferrous metals in the metal concentrate.

Table 6. Results of the Smelting Tests on Two 2–6 mm Aluminum Samples and One 2–15 mm Sample

Sample	1	2	3
Size	2–6 mm	2–6 mm	2–15 mm
Cryolite added	10%	15%	10%
Sample weight	30 g	30 g	30 g
Metal weight	23.0 g	23.4 g	23.7 g
Smelt recovery	76.5%	78%	79%

CONCLUSION

Magnus separation is a novel type of eddy current separation that can recover fine metal particles from solid waste. Among the potential applications are the wet separation of aluminum and heavy nonferrous metals from the fine fraction of bottom ash and the recovery of precious metals from dry alluvial deposits.

ACKNOWLEDGMENTS

The authors are grateful to Dr. A. Weisenborn of Shell for his overview of the literature on the Magnus effect and to Mr. P. A. C. M. Haeser for his experiments on the Magnus effect in air.

REFERENCES

1. RIVM website www.rivm.nl, sheet C14.6: Composition of Non-separated Household Waste and Sheet A7.7: Incineration Installations.
2. McKinsey & Company. Towards an Improved Cycle for Aluminium, Report 1994/13, VROM, Zoetermeer, 1993; 41.
3. Rem, P.C. *Eddy Current Separation*; ISBN 90-5166-702-8; Eburon: Delft, 1999; 123.
4. Dutch Patent 1010977, 1999.
5. Tritton, D.J. *Physical Fluid Dynamics*, 2nd Ed.; ISBN 0-19-854489-8; Clarendon: Oxford, 1988; 159.
6. Magnus, G. Über die Abweichung der Geschosse. Berl. Abhandlungen (Phys. Kl.) **1852**, 1–2.
7. Barkla, H.M.; Auchterlonie, L.J. The Magnus or Robins Effect on Rotating Spheres. J. Fluid Mech. **1971**, *47*, 437–447.

8. Flettner, A. *Mein Weg zum Rotor*; Koehler & Amelang: Leipzig, 1926; 103.
9. Davies, J.M. The Aerodynamics of Golf Balls. J. Appl. Phys. **1949**, *20*, 821–828.
10. Maccoll, J.W. Aerodynamics of a Spinning Sphere. J. R. Aeron. Soc. **1928**, *32*, 777–798.

Received September 2001
Revised January 2002